Inorg. Chem. **2002**, *41*, 5566–5574

Synthesis, Structures, and Magnetic and Optical Properties of a Series of Europium(III) and Gadolinium(III) Complexes with Chelating Nitronyl and Imino Nitroxide Free Radicals

Christophe Lescop,[†,‡] Dominique Luneau,*[,†,§] Paul Rey,[†] Guillaume Bussière,[⊥] and Christian Reber*[,⊥]

Laboratoire de Chimie Inorganique et Biologique (UMR 5046), DRFMC, CEA-Grenoble, 17 Rue des Martyrs, 38054 Grenoble Cedex 09, France, and Département de Chimie, Université de Montréal, Montréal, QC H3C 3J7, Canada

Received June 13, 2002

This paper reports the synthesis, structures, and magnetic and optical properties of a series of gadolinium(III) (**1a**–**4a**) and europium(III) (**1b**–**4b**) complexes with nitronyl or imino nitroxide radicals. The crystal structures of compounds **1a** and **1b** consist of $[Ln^{III}(radical)_2(NO_3)_3]$ entities in which the gadolinium(III) (**1a**) or europium(III) ion (**1b**) is 10-coordinated to two nitronyl nitroxide radicals and three nitrato ligands. The crystal structures of compounds **2a**–**4a** and **2b**–**4b** consist of $[Ln^{III}(hfac)_3(radical)]$ entities in which the gadolinium(III) (**2a**–**4a**) or europium(III) ion (**2b**–**4b**) is 8-coordinated to one nitronyl (**2a** and **2b**) or one imino (**3a**, **4a** and **3b**, **4b**) nitroxide radical and three hexafluoroacetylacetonato ligands. The gadolinium(III) complexes (**1a**–**4a**) are isostructural with their europium(III) analogues (**1b**–**4b**). The magnetic properties of the gadolinium complexes were studied. Along the series **1a**–**4a** only compound **2a** exhibits a ferromagnetic Gd^{III}–radical coupling ($J_{Gd-rad} = +1.7$ cm^{-1}), while for the others this coupling is antiferromagnetic (**1a**: $J_{Gd-rad1} = -4.05$ cm^{-1} and $J_{Gd-rad2} = -0.80$ cm^{-1}; **3a**: $J_{Gd-rad} = -2.6$ cm^{-1}; **4a**: $J_{Gd-rad} = -1.9$ cm^{-1}). The first full luminescence spectra of lanthanide complexes with free radical ligands are reported between 650 and 1200 nm. The rich vibronic structure in luminescence and absorption spectra indicates that several excited states define the absorption spectra between 400 and 800 nm. Qualitative trends can be established between magnetic ground state properties and the energies and fine structure of the title compounds.

Introduction

Research in the field of molecular based magnetic materials has led to various systems exhibiting spontaneous magnetization[1−5] but also single-molecule magnet properties,[6] spin transitions,[7] photomagnetism,[8−11] or chiral magnetism.[12,13] To date, most of the appealing results in this field rely on coordination compounds of the first-row transition metal ions. In contrast, molecular magnetic materials based on rare earth metal ions are less numerous despite their interesting optical properties, which could lead to materials with novel optical and magnetic properties.[14]

* Corresponding authors. E-mail: dominique.luneau@univ-lyon1.fr; reber@chimie.umontreal.ca.
† Laboratoire de Chimie Inorganique et Biologique.
‡ Present address: Organométalliques et Catalyse: Chimie et Electrochimie Moléculaires, UMR 6509, Institut de Chimie de Rennes, CNRS, Université de Rennes 1, Campus de Beaulieu, 35042 Rennes Cedex, France.
§ Present address: Université Claude Bernard Lyon I, Bât 305, 43 Avenue du 11 Novembre 1918, 69622 Villeurbanne Cedex, France.
⊥ Université de Montréal.

(1) Luneau, D. *Curr. Opin. Solid State Mater. Sci.* **2001**, *5*, 123.
(2) Miller, J. S.; Epstein, A. J. *MRS Bull.* **2000**, *25*, 21.
(3) Ovcharenko, V. I.; Sagdeev, R. Z. *Russ. Chem. Rev.* **1999**, *68*, 345.
(4) Verdaguer, M.; Bleuzen, A.; Marvaud, V.; Vaissermann, J.; Seuleman, M.; Desplanches, C.; Scuiller, A.; Train, C.; Garde, R.; Gelly, G.; Lomenech, C.; Rosenman, I.; Veillet, P.; Cartier, C.; Villain, F. *Coord. Chem. Rev.* **1999**, *190*−*192*, 1023.
(5) Ouahab, L. *Chem. Mater.* **1997**, *9*, 1909.
(6) Gatteschi, D.; Sessoli, R.; Cornia, A. *Chem. Commun.* **2000**, 725.
(7) Gütlich, P.; Garcia, Y.; Goodwin, H. *Chem. Soc. Rev.* **2000**, *29*, 419.
(8) Sato, O.; Iyoda, T.; Fujishima, A.; Hashimoto, K. *Science* **1996**, *272*, 704.
(9) Pejakovic, D. A.; Manson, J. L.; Miller, J. S.; Epstein, A. J. *J. Appl. Phys.* **2000**, *87*, 6028.
(10) Matsuda, K.; Irie, M. *J. Am. Chem. Soc.* **2000**, *122*, 7195.
(11) Bleuzen, A.; Lomenech, C.; Escax, V.; Villain, F.; Varret, F.; Cartier dit Moulin, C.; Verdaguer, M. *J. Am. Chem. Soc.* **2000**, *122*, 6648.
(12) Minguet, M.; Luneau, D.; Lhotel, E.; Villar, V.; Paulsen, C.; Amabilino, D. B.; Veciana, J. *Angew. Chem., Int. Ed.* **2002**, *41*, 586.
(13) Andrés, R.; Brissard, M.; Gruselle, M.; Train, C.; Vaissermann, J.; Malézieux, B.; Jamet, J.-P.; Verdaguer, M. *Inorg. Chem.* **2001**, *40*, 4633.
(14) Benelli, C.; Gatteschi, D. *Chem. Rev.* **2002**, *102*, 2369.

10.1021/ic0257928 CCC: $22.00
Published on Web 09/27/2002

In this context, and as a part of our research program on the magnetism of metal−radical coordination compounds, we have investigated lanthanide−radical complexes. An unexpected result of this work was the elucidation of the first antiferromagnetic Gd^{III}−radical interaction.[15] Prior to our report, the magnetic interaction between gadolinium(III) and free radical ligands,[16−20] or Cu(II)[21−30] and vanadium(II) ions,[28] was assumed to be intrinsically ferromagnetic. This was understood as a consequence of electron transfer integrals involving the magnetic orbital of the free radical (π), or those of the metal ion (d), and the empty orbitals of the gadolinium(III) ion (5d or 6s) that stabilized the higher multiplicity ground spin state following Hund's rule.[21,26] Following new investigations by us and others, either for Gd(III)−radical or Gd(III)−Cu(II) complexes, this model is now no longer universally applicable.[14,31,32]

In an effort to understand the factors that govern the sign of the magnetic coupling in such systems, we synthesized several series of lanthanide−radical complexes with a variable number of different radical ligands coordinated to the metal center. We recently reported the synthesis and magnetic properties of a series of gadolinium complexes which all exhibit antiferromagnetic Gd^{III}−radical interactions.[33] These results underline that the sign of the Gd^{III}−radical interaction, ferro- or antiferromagnetic, depends on the type of radical and to some extent on the nature of the ancillary ligands involved in the coordination sphere of the gadolinium. In the present study, optical spectroscopy measurements are reported in order to gain a better description of the electronic structure of these compounds, a first step toward a correlation of magnetic and optical properties. Very recently, a related study concerning some lanthanide(III) complexes with the imino-nitroxide radical IMPy (**7**) was also reported by Kaizaki et al.[34]

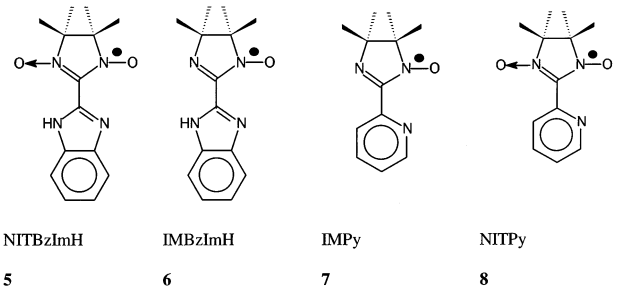

Figure 1. Schematic representations of the nitronyl nitroxides radicals NITBzImH **5** (complexes **1a**, **1b**, **2a**, and **2b**) and NITPy **8** and of the imino nitroxide radicals IMBzImH **6** (complexes **3a** and **3b**) and IMPy **7** (complexes **4a** and **4b**).

We report the synthesis and crystal structures of a series of gadolinium(III) complexes, and their europium(III) analogues, with nitronyl-nitroxide (NITBzImH, **5**) and imino-nitroxide radicals (IMBzImH) **6** and (IMPy) **7** (Figure 1). The latter are among the rare examples of lanthanide complexes with imino-nitroxide radicals. The studies of the magnetic behaviors of the gadolinium complexes reveal that only one complex among the series exhibits a ferromagnetic Gd^{III}−radical interaction, while for the other gadolinium(III) complexes this interaction is unambiguously antiferromagnetic.

Absorption and emission spectra of these compounds are also reported and analyzed. In the case of the europium(III) complexes, an unprecedented phenomenon of competition between ligand-centered luminescence and metal-centered f−f luminescence is observed. Comparative analyses of these spectra show the subtle changes that contribute to the delicate balance that exists between ferromagnetism and antiferromagnetism in such systems. The study of the optical properties of such complexes reveals pertinent information in order to investigate effects defining their magnetism, but also illustrates the rich electronic structure of the title compounds, which leads to new absorption and luminescence properties for these magnetic materials.

Experimental Section

Radical Synthesis. Nitronyl nitroxide radicals 2,3-bis(hydroxylamino)-2,3-dimethylbutane-2-(2′-benzymidazolyl)-4,4,5,5-tetramethylimidazoline-1-oxyl-3-oxide (NITBzImH, **5**) and 2,3-bis(hydroxylamino)-2,3-dimethylbutane-2-(2′-pyridinyl)-4,4,5,5-tetramethylimidazoline-1-oxyl-3-oxide (NITPy, **8**), and the corresponding imino nitroxide radicals 2,3-bis(hydroxylamino)-2,3-dimethylbutane-2-(2′-benzymidazolyl)-4,4,5,5-tetramethylimidazoline-1-oxide (IMBzImH, **6**) and 2,3-bis(hydroxylamino)-2,3-dimethylbutane-2-(2′-pyridinyl)-4,4,5,5-tetramethylimidazoline-1-oxide (IMPy, **7**), were synthesized according to literature methods.[35,36] The starting complexes $Ln(hfac)_3{\cdot}2H_2O$ (Ln = Eu and Gd) were also synthesized

(15) Lescop, C.; Luneau, D.; Belorizky, E.; Fries, P.; Guillot, M.; Rey, P. *Inorg. Chem.* **1999**, *38*, 5472.
(16) Benelli, C.; Caneschi, A.; Gatteschi, D.; Laugier, J.; Rey, P. *Angew. Chem., Int. Ed. Engl.* **1987**, *26*, 913.
(17) Benelli, C.; Caneschi, A.; Gatteschi, D.; Pardi, L.; Rey, P. *Inorg. Chem.* **1989**, *28*, 275.
(18) Benelli, C.; Caneschi, A.; Gatteschi, D.; Pardi, L.; Rey, P. *Inorg. Chem.* **1990**, *29*, 4223.
(19) Benelli, C.; Caneschi, A.; Gatteschi, D.; Pardi, L. *Inorg. Chem.* **1992**, *31*, 741.
(20) Sutter, J.-P.; Kahn, M. L.; Golhen, S.; Ouahab, L.; Kahn, O. *Chem. Eur. J.* **1998**, *4*, 571.
(21) Benelli, C.; Caneschi, A.; Gatteschi, D.; Guillou, O.; Pardi, L. *Inorg. Chem.* **1990**, *29*, 1750.
(22) Bencini, A.; Benelli, C.; Caneschi, A.; Carlin, R. L.; Dei, A.; Gatteschi, D. *J. Am. Chem. Soc.* **1985**, *107*, 8128.
(23) Costes, J.-P.; Dahan, F.; Dupuis, A. *Inorg. Chem.* **2000**, *39*, 165.
(24) Benelli, C.; Fabretti, A. C.; Giusti, A. *J. Chem. Soc., Chem. Commun.* **1993**, 409.
(25) Guillou, O.; Bergerat, P.; Kahn, O.; Bakalbassis, E.; Boubeker, K.; Batail, P.; Guillot, M. *Inorg. Chem.* **1992**, *31*, 110.
(26) Andruh, M.; Ramade, I.; Godjovi, E.; Guillou, O.; Kahn, O.; Trombe, J.-C. *J. Am. Chem. Soc.* **1993**, *115*, 1822.
(27) Sanz, J. L.; Ruiz, R.; Gleizes, A.; Lloret, F.; Faus, J.; Julve, M.; Borras-Almenar, J. J.; Journaux, Y. *Inorg. Chem.* **1996**, *35*, 7384.
(28) Costes, J.-P.; Dupuis, A.; Laurent, J.-P. *J. Chem. Soc., Dalton Trans.* **1998**, 735.
(29) Sakamoto, M.; Hashimura, M.; Matsuki, K.; Matsumoto, N.; Inoue, K.; Okawa, H. *Bull. Chem. Soc. Jpn.* **1991**, *64*, 3639.
(30) Matsumoto, N.; Sakamoto, M.; Tamaki, H.; Okawa, H.; Kida, S. *Chem. Lett.* **1990**, 853.
(31) Caneschi, A.; Dei, A.; Gatteschi, D.; Sorace, L.; Vostrikova, K. E. *Angew. Chem., Int. Ed.* **2000**, *39*, 246.
(32) Costes, J.-P.; Dahan, F.; Dupuis, A.; Laurent, J.-P. *Inorg. Chem.* **2000**, *39*, 169.
(33) Lescop, C.; Belorizky, E.; Luneau, D.; Rey, P. *Inorg. Chem.* **2002**, *41*, 3375.
(34) Tsukuda, T.; Suzuki, T.; Kaizaki, S. *J. Chem. Soc., Dalton Trans.* **2002**, 1721.
(35) Ullman, E. F.; Osiecky, J. H.; Boocock, D. G. B.; Darcy, R. *J. Am. Chem. Soc.* **1972**, *94*, 7049.
(36) Fegy, K.; Luneau, D.; Ohm, T.; Paulsen, C.; Rey, P. *Angew. Chem., Int. Ed.* **1998**, *37*, 1270.

as reported in the literature.[37] Other reactants were used as purchased.

Complex Synthesis. In the following **1a**, **2a**, **3a**, and **4a** hold for the gadolinium(III) complexes, while **1b**, **2b**, **3b**, and **4b** hold for the europium(III) complexes.

[Ln^{III}(radical)$_2$(NO_3)$_3$] (radical = NITBzImH, **5**): **1a** and **1b** were synthesized as previously described with yields superior to 65% from ethanolic solutions containing 1 equiv of [Ln(NO_3)$_3$·6H_2O] and 2 equiv of the radical NITBzImH **5**.[33,38]

[Ln^{III}(hfac)$_3$radical], **2a** and **2b** (radical = NITBzImH, **5**), **3a** and **3b** (radical = IMBzImH, **6**), and **4a** and **4b** (radical = IMPy, **7**) were obtained following the same procedure: 1 equiv of [Ln(hfac)$_3$·2H_2O] was dissolved in hot heptane and then mixed with a solution of 1 equiv of radical in chloroform. The resulting clear solution, blue in the case of nitronyl-nitroxide radical and red for the imino-nitroxide radicals, was allowed to stand at room temperature for 2 days to produce well-shaped dark blue (**2a** and **2b**) or red-orange crystals (**3a**, **3b**, **4a**, **4b**). **2a**: yield = 57%, mp = 125−7 °C; **2b**: yield = 65%; **3a**: yield = 51%, mp = 170−3 °C; **3b**: yield = 60%; **4a**: yield = 45%, mp = 135−8 °C; **4b**: yield = 73%. Elemental analyses were satisfactory. Anal. Calcd for (**2a**) $C_{29}H_{20}N_4F_{18}O_8Gd$: C 33.1, H 1.9, N 5.3, Gd 15.0. Found: C 33.1, H 1.8, N 5.3, Gd 15.5. Anal. Calcd for (**2b**) $C_{29}H_{20}N_4F_{18}O_8Eu$: C 33.3, H 1.9, N 5.4, Eu 14.5. Found: C 33.4, H 1.9, N 5.4, Eu 13.7. Anal. Calcd for (**3a**) $C_{29}H_{20}N_4F_{18}O_7Gd$: C 33.6, H 1.9, N 5.4, Gd 15.2. Found: C 33.8, H 1.9, N 5.4. Anal. Calcd for (**3b**) $C_{29}H_{20}N_4F_{18}O_7Eu$: C 33.8, H 2.0, N 5.4, Eu 14.7. Found: C 33.9, H 2.0, N 5.4, Eu 13.9. Anal. Calcd for (**4a**) $C_{27}H_{19}N_3F_{18}O_7Gd$: C 32.5, H 1.9, N 4.2, Gd 15.8. Found: C 32.9, H 1.7, N 4.1, Gd 15.9. Anal. Calcd for (**4b**) $C_{27}H_{19}N_3F_{18}O_7Eu$: C 32.7, H 1.9, N 4.2, Eu 15.3. Found: C 32.9, H 1.9, N 4.2, Eu 14.5.

X-ray Crystallography. Data were collected on a BRUKER SMART CCD diffractometer equipped with a normal focus monochromatized molybdenum-target X-ray tube and were processed for reduction and absorption through the SAINT software.[39] Structures were solved with the SHELXTL software.[40] All nonhydrogen atoms were refined with anisotropic thermal parameters. The hydrogen atoms were included in the final refinement model in calculated positions with isotropic thermal parameters. Crystal structure and refinement data are summarized in Table 1 for the gadolinium compounds **2a**−**4a** and in Table 2 for the europium compounds **2b**−**4b**. Data for compounds **1a** and **2a** were previously reported.[33]

2a: MW = 1051.74, dark blue parallelipipedal, orthorhombic, space group *Pbca* (No. 61), a = 20.7769(9) Å, b = 16.4918(7) Å, c = 23.1570(9) Å, Z = 8, V = 7934.7(6) Å^3, 14 544 reflections measured, 3520 independent reflections (R_{int} = 0.0406), $R(F)$ = 0.0256 ($I > 2\sigma(I)$), $wR(F^2)$ = 0.0871 (all data); **2b**: MW = 1046.45, dark blue parallelipipedal, orthorhombic, space group *Pbca* (No. 61), a = 20.8076(8) Å, b = 16.8121(7) Å, c = 23.3231(9) Å, Z = 8, V = 8158.9(6) Å^3, 50 737 reflections measured, 10 201 independent reflections (R_{int} = 0.0806), $R(F)$ = 0.0407 ($I > 2\sigma(I)$), $wR(F^2)$ = 0.1101 (all data); **3a**: MW = 1035.74, red parallelipipedal, monoclinic, space group *P*21/*n* (No. 14), a = 11.4160(14) Å, b = 21.877(3) Å, c = 16.1879(19) Å, β = 108.795(2)°, Z = 4, V = 3827.4(8) Å^3, 24 449 reflections measured, 9246 independent reflections (R_{int} = 0.1044), $R(F)$ = 0.0511 ($I > 2\sigma(I)$), $wR(F^2)$ = 0.1515 (all data); **3b**: MW = 1030.45, red parallelipipedal, monoclinic, space group *P*21/*n* (No. 14), a = 11.5570(5) Å, b = 21.9488(10) Å, c = 16.3080(8) Å, β = 108.3890(10)°, Z = 4, V = 3925.5(3) Å^3, 25 122 reflections measured, 9500 independent reflections (R_{int} = 0.0447), $R(F)$ = 0.0295 ($I > 2\sigma(I)$), $wR(F^2)$ = 0.0630 (all data); **4a**: MW = 996.70, orange prism, monoclinic, space group *P*21/*n* (No. 14), a = 9.4053(5) Å, b = 31.3293(16) Å, c = 12.1898(6) Å, β = 98.4610(10)°, Z = 4, V = 3552.8(3) Å^3, 22 646 reflections measured, 8638 independent reflections (R_{int} = 0.0415), $R(F)$ = 0.0517 ($I > 2\sigma(I)$), $wR(F^2)$ = 0.1809 (all data); **4b**: MW = 991.41, orange prism, monoclinic, space group *P*21/*n* (No. 14), a = 9.6171(14) Å, b = 31.574(5) Å, c = 12.2073(17) Å, β = 98.736(3)°, Z = 4, V = 3663.7(9) Å^3, 23 419 reflections measured, 8906 independent reflections (R_{int} = 0.0384), $R(F)$ = 0.0427 ($I > 2\sigma(I)$), $wR(F^2)$ = 0.1255 (all data).

Magnetic Measurements. The temperature dependence of the magnetic susceptibilities for the gadolinium complexes was measured on bulk crystalline materials with a Quantum Design MPMS superconducting SQUID magnetometer operating at a field strength of 0.5 T and in the temperature range 2−300 K. Measurements of the magnetic field dependence of the magnetization were performed on the same magnetometer at 2 K and in the field range 0−5.5 T.

Table 1. Summary of Crystallographic Data for the Gadolinium(III) Compounds **2a**−**4a**

	2a	**3a**	**4a**
formula	$C_{29}H_{20}N_4F_{18}O_8Gd$	$C_{29}H_{20}N_4F_{18}O_7Gd$	$C_{27}H_{19}N_3F_{18}O_7Gd$
fw	1051.74	1035.74	996.70
T (K)	193(2)	193(2)	298(2)
cryst syst	orthorhombic	monoclinic	monoclinic
space group	*Pbca*	*P*2$_1$/*n*	*P*2$_1$/*n*
a (Å)	20.7769(9)	11.416(1)	9.4053(5)
b (Å)	16.4918(7)	21.877(3)	31.329(2)
c (Å)	23.1570(9)	16.188(2)	12.1898(6)
β (deg)	90	108.795(2)	98.461(1)
V (Å^3)	7934.7(6)	3827.4(8)	3552.8(3)
Z	8	4	4
μ (mm^{-1})	2.032	1.869	2.008
ρ_{calcd} (cm^3)	1.981	1.797	1.863
λ (Å)	0.71073	0.71073	0.71073
$R(F)^a$ $I > 2\sigma(I)$	0.0314	0.0522	0.0517
$R_w(F^2)^b$ all data	0.1081	0.1542	0.1809

^{a} $R(F) = \sum||F_o| - |F_c||/\sum|F_o|$, $R_w(F^2) = \sum[w(F_o^2 - F_c^2)^2/\sum wF_o^4]^{1/2}$.

Table 2. Summary of Crystallographic Data for the Europium(III) Compounds **2b**−**4b**

	2b	**3b**	**4b**
formula	$C_{29}H_{20}N_4F_{18}O_8Eu$	$C_{29}H_{20}N_4F_{18}O_7Eu$	$C_{27}H_{19}N_3F_{18}O_7Eu$
fw	1729.10	1030.45	991.41
T (K)	298(2)	298(2)	298(2)
cryst syst	orthorhombic	monoclinic	monoclinic
space group	*Pbca*	*P*2$_1$/*n*	*P*2$_1$/*n*
a (Å)	20.8076(8)	11.5570(5)	9.6171(14)
b (Å)	16.8121(7)	21.9488(10)	31.574(5)
c (Å)	23.3231(9)	16.3080(8)	12.2073(17)
β (deg)	90	108.389(1)	98.736(3)
V (Å^3)	8158.9(6)	3925.5(3)	3663.7(9)
Z	8	4	4
μ (mm^{-1})	1.668	1.730	1.849
ρ_{calcd} (cm^3)	1.704	1.744	1.797
λ (Å)	0.71073	0.71073	0.71073
$R(F)^a$ $I > 2\sigma(I)$	0.0407	0.0295	0.0427
$R_w(F^2)^b$ all data	0.1101	0.0630	0.1255

^{a} $R(F) = \sum||F_o| - |F_c||/\sum|F_o|$, $R_w(F^2) = \sum[w(F_o^2 - F_c^2)^2/\sum wF_o^4]^{1/2}$.

(37) Richardson, M. F.; Wagner, D. F.; Sands, D. E. *J. Inorg. Nucl. Chem.* **1968**, *30*, 1275.
(38) Lescop, C.; Luneau, D.; Bussière, G.; Triest, M.; Reber, C. *Inorg. Chem.* **2000**, *39*, 3740.
(39) *SAINT*; 4.050 ed.; Bruker Analytical X-ray Instruments, Inc.: Madison, WI, 1998.
(40) *SHELXTL*; 5.030 ed.; Brucker Analytical X-ray Instruments, Inc.: Madison, WI, 1998.

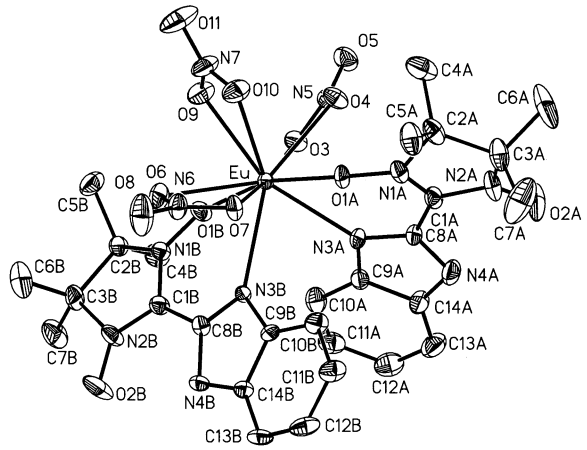

Figure 2. View of the complex $[Eu^{III}(NITBzImH)_2(NO_3)_3]$ (**1b**) with atom labeling and ellipsoids at 30% probability. Hydrogen atoms have been omitted for clarity.

The data were corrected for diamagnetism of the constituent atoms using Pascal constants.

Optical Spectroscopy. All spectra were measured with instruments described in detail previously.[41,42] Absorption measurements were carried out with a Varian Cary 5E spectrometer with the sample cooled in an Oxford Instruments CF-1204 He gas flow cryostat. Luminescence measurements were made either with a Renishaw System 3000 Raman microscope using the 514.5 nm line of an Ar ion laser as excitation source or with a locally built luminescence setup using a 150 W Xe arc lamp as excitation source and a Spex 1800-II monochromator with an ADC 403L Ge detector to scan the spectrum. The correction for the wavelength-dependent sensitivity of this instrument has been described before.[42] The latter instrument is less sensitive, but its range extends into the near-infrared to 1800 nm, whereas the highly sensitive microscope does not allow intensity at wavelengths beyond approximately 950 nm to be detected.

Results

Crystal Structures. Each of the gadolinium(III) complexes (**1a**, **2a**, **3a**, and **4a)** was found isostructural with the corresponding europium(III) analogue (**1b**, **2b**, **3b**, and **4b)**. Views of the molecular structure for compounds **1b** and **2a** are shown in Figures 2 and 3. Selected bond lengths and angles are listed in Table 3 for compounds **2a**−**4a** and **2b**−**4b**.

$[Ln^{III}(NITBzImH)_2(NO_3)_3]$ (1a and 1b). These two complexes were described in our previous papers.[33,38] We recall hereafter the main structural features. The europium(III) and gadolinium(III) complexes **1a** and **1b** are isostructural and crystallize in the noncentrosymmetric space group $Pna2_1$. A view of the europium complex (**1b**) is shown in Figure 2. The lanthanide ion is 10-coordinated by three η^2-nitrato anions and two radicals (NITBzImH, **5**) in a chelating way involving one oxygen atom (O1A and O1B) of the nitronyl nitroxide moiety and one nitrogen atom (N3A and N3B) of the benzimidazole substituent. The differences in bond lengths between the europium complex (Eu−O1A 2.369(5) Å, Eu−O1B 2.413(5) Å; Eu−N3A 2.590(7) Å; Eu−N3B 2.598(6) Å) and the gadolinium complex (Gd−O1A 2.405(3) Å, Gd−O1B 2.365(3) Å; Gd−N3A 2.613(3) Å; Gd−N3B 2.585(3) Å) are in agreement with the lanthanide contraction. The shortest intermolecular distances (>3.40 Å) are found between the uncoordinated groups of the nitronyl nitroxide ligands [O2A- - -O2Bi 3.343(5) Å, O2A- - -N2Bi

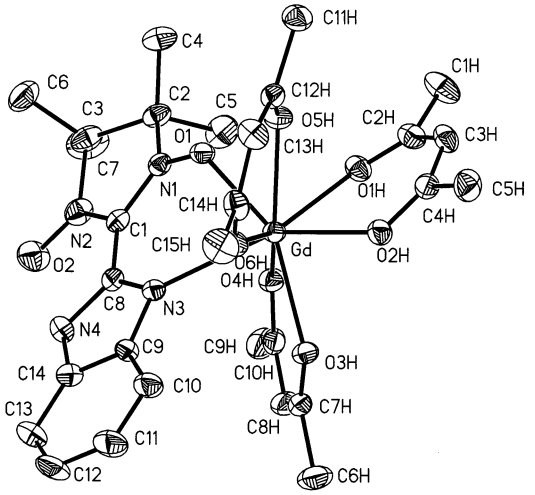

Figure 3. View of the complex $[Gd^{III}(hfac)_3$ NITBzImH] (**2a**) with atom labeling and ellipsoids at 30% probability. Hydrogen and fluorine atoms have been omitted for clarity.

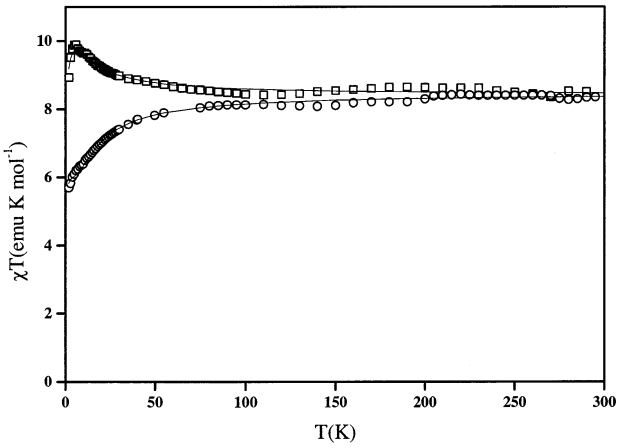

Figure 4. Temperature dependence of $\chi_m T$ for $[Gd^{III}(hfac)_3$NITBzImH] (**2a**) (squares) and for $[Gd^{III}(hfac)_3$ IMBzImH] (**3a**) (circles). Solid lines are calculated with the parameters reported in the text.

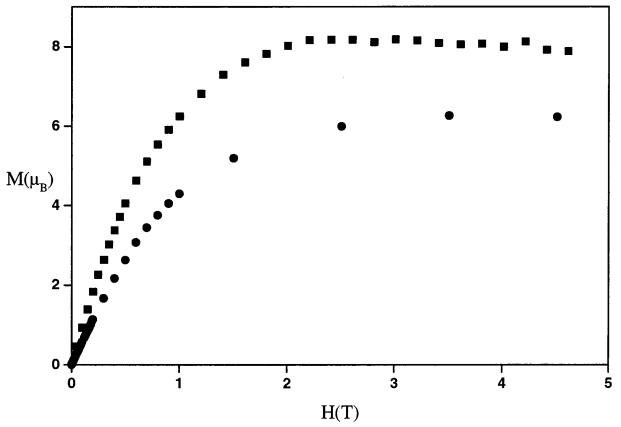

Figure 5. Magnetic field dependence of the magnetization at 2 K for $[Gd^{III}(hfac)_3$NITBzImH] (**2a**) (squares) and for $[Gd^{III}(hfac)_3$ IMBzImH] (**3a**) (circles).

(41) Bussière, G.; Beaulac, R.; Cardinal-David, B.; Reber, C. *Coord. Chem. Rev.* **2001**, *219*−*221*, 509.
(42) Davis, M. J.; Reber, C. *Inorg. Chem.* **1995**, *34*, 4585.

Table 3. Selected Bond Lengths (Å) and Angles (deg) for the Gadolinium(III) Complexes **2a**−**4a** and for the Europium(III) Complexes **2b**−**4b**

	2a (Ln = Gd)	**2b** (Ln = Eu)	**3a** (Ln = Gd)	**3b** (Ln = Eu)	**4a** (Ln = Gd)	**4b** (Ln = Eu)
Ln−O1	2.342(3)	2.359(3)				
Ln−N1			2.599(5)	2.621(2)	2.555(4)	2.557(2)
Ln−N3	2.570(3)	2.593(3)	2.519(5)	2.533(2)	2.557(4)	2.568(2)
O1−N1	1.286(4)	1.287(4)				
O2−N2	1.273(4)	1.272(5)	1.261(7)	1.255(3)	1.269(6)	1.273(4)
N1−Ln−N3	71.48(10)	70.9(1)	66.0(2)	65.80(7)	64.5(1)	64.12(7)

3.443(5) Å, and N2A- - -O2Bi 3.832(5) Å (**1a**); O2A- - -O2Bi 3.32(1) Å, O2A- - -N2Bi 3.42(1) Å, and N2A- - -O2Bi 3.81(1) Å (**1b**)]. No other short intermolecular contacts are observed between atoms carrying high spin densities (i.e., the lanthanide(III) ion and the O1−N1−C1−N2−O2 nitronyl-nitroxide moiety).

[Ln^{III}(hfac)$_3$NITBzImH] (2a and 2b). Complexes **2a** and **2b** are isostructural and crystallize in the orthorhombic *Pbca* space group. The lanthanide ion is coordinated to one nitronyl nitroxide radical through a chelate involving one oxygen atom (O1) of the NO groups and one nitrogen atom (N3) of the benzimidazole moiety as observed for **1a** and **1b**. The coordination sphere is filled at eight by the six oxygen atoms of the three ancillary hexafluoroacetylacetonate (hfac) ligands. A view of the gadolinium complex (**2a)** is shown in Figure 3. As for **1a** and **1b** the differences in bond lengths between the europium complex (Eu−O1 2.359(3) Å, Eu−N3 2.595(4) Å) and the gadolinium complex (Gd−O1 2.342(3) Å, Gd−N3 2.570(3) Å) are also in agreement with the lanthanide contraction (Table 3). For the gadolinium complex these structural features compare well with those found for the gadolinium complex of the pyridinyl-substituted nitronyl nitroxide (NITPy, **8**) (Figure 1).[19] In the crystal, the shortest intermolecular contacts involving atoms carrying high spin densities are observed between the lanthanide ion and the uncoordinated O2 oxygen atom of the radical of the neighboring complex and are quite long (>3.9 Å).

[Ln^{III}(hfac)$_3$IMBzImH] (3a and 3b) and [Ln^{III}(hfac)$_3$IMPy] (4a and 4b). Complexes **3a**, **3b**, **4a**, and **4b** crystallize in the monoclinic space group *P*21/*n*. The crystal structures of some lanthanide IMPy complexes were also reported recently by others.[34] The lanthanide ion is coordinated to one imino-nitroxide ligand through a chelate involving the imino nitrogen atom (N1) of the imino-nitroxide moiety and the pyridinyl nitrogen atom (N3) of the benzimidazolyl (**3a**, **3b**) or pyridinyl (**4a**, **4b**) substituent. The coordination sphere is filled to eight by the six oxygen atoms of the three ancillary hexafluoroacetylacetonate ligands (hfac). As observed for the other complexes, the differences in bond lengths between the europium complex [Eu−N1 2.620(2) Å (**3b**), Eu−N1 2.556(2) Å (**4b**), Eu−N3 2.533(2) Å (**3b**), Eu−N3 2.568(2) Å (**4b**)] and the gadolinium complex [Gd−N1 2.599(5) Å (**3a**), Gd−N1 2.555(2) Å (**4a**), Gd−N3 2.519(5) Å (**3a**), Gd−N3 2.557(4) Å (**4a**)] hold for the lanthanide contraction (Table 3).

Close examination of the crystal packing in **3a** and **4a** shows no short intermolecular contact (<5 Å) involving atoms carrying high spin densities (i.e., lanthanide(III) ion and N1−C1−N2−O1 imino-nitroxide moiety).

Magnetic Properties. This section describes the magnetic properties of the gadolinium(III) complexes **1a**, **2a**, **3a**, and **4a**.

[Gd^{III}(NITBzImH)$_2$(NO$_3$)$_3$] (1a). The magnetic behavior of this complex was fully detailed and analyzed in a previous publication.[33] The Gd^{III}−radical interactions were found unambiguously antiferromagnetic. More precisely the fitting of the temperature dependence of the magnetic susceptibility required two different antiferromagnetic Gd^{III}−radical couplings accounting for both radicals bound to the gadolinium(III) ion ($J_{Gd-rad1} = -4.05(3)$ cm^{-1} and $J_{Gd-rad2} = -0.80$ cm^{-1}).

[Gd^{III}(hfac)$_3$NITBzImH] (2a). The temperature dependence of the molar magnetic susceptibility χ is presented in Figure 4 in the form of the product of the magnetic susceptibility χ with the temperature (χT) versus the temperature T. At 300 K χT (8.40 emu K mol^{-1}) is close to the value expected for one gadolinium(III) ($S = 7/2$) and one radical ($S = 1/2$) magnetically independent (8.25 emu K mol^{-1}). Upon cooling, χT keeps almost constant until 80 K, then slowly increases and reaches a maximum (9.9 emu K mol^{-1}) at 6 K. Afterward χT decreases continuously. Such a magnetic behavior is characteristic of dominant ferromagnetic interactions operant in **2a**. These data were analyzed by a refinement program[43] which numerically diagonalizes the isotropic Hamiltonian ($H = -2\sum_{i<j} J_{ij}S_iS_j$) considering one Gd^{III}−radical interaction (J_{Gd-rad}). An additional intermolecular interaction (zJ), treated in the mean field approximation, was included to take into account the decrease at low temperature. A good fit of the experimental data (Figure 4) was obtained with $g = 2.02$; $J_{Gd-rad} = +1.7$ cm^{-1} and $zJ = -0.01$ cm^{-1} with $R = 5\ 10^{-5}$ [$R = \sum(\chi T_{obs} - \chi T_{calc})^2/\sum(\chi T_{obs})^2$]. Furthermore, magnetization measurements versus magnetic field reach a saturation value close to 8 μ_B at 2 K (Figure 5), which corresponds well to the value expected for a ground state with a spin multiplicity $S = 4$ in the case of one gadolinium(III) and one radical ferromagnetically coupled. Moreover, the Gd^{III}−radical exchange coupling $J_{Gd-rad} = +1.7$ cm^{-1} is comparable with those (+1.5 cm^{-1}) found for the gadolinium complex of the pyridinyl-substituted nitronyl nitroxide radical [Gd^{III}(hfac)$_3$NITPy].[19]

[Gd^{III}(hfac)$_3$IMBzImH] (3a) and [Gd^{III}(hfac)$_3$IMPy] (4a). The two compounds exhibit similar magnetic behaviors. The results are presented for **3a** in Figure 4 as χT vs T. These are in agreement with other reports.[34] At room temperature both complexes present χT values (8.30 emu K mol^{-1} for

(43) Belorizky, E.; Fries, P. H.; Gojon, E.; Latour, J.-M. *Mol. Phys.* **1987**, *61*, 661.

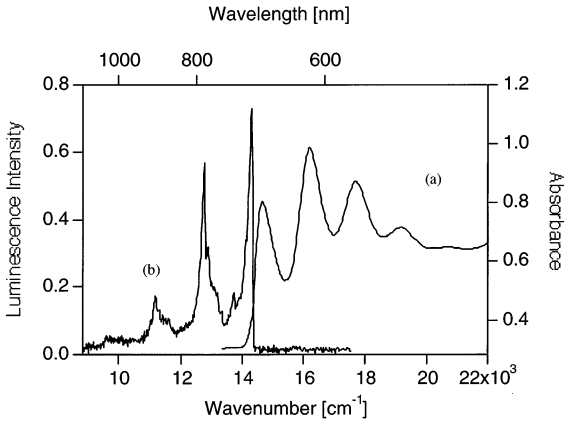

Figure 6. Single-crystal absorption (a) and luminescence (b) spectra of [$Gd^{III}(hfac)_3$NITBzImH] (**2a**) at 5 K.

3a and **4a**) that are, as for **2a**, in agreement with noninteracting $S = 7/2$ and $S = 1/2$ spins (8.25 emu K mol^{-1}). Upon cooling, χT keeps almost constant down to 50 K, then decreases continuously. Such a magnetic behavior is consistent with dominant antiferromagnetic interactions in both compounds. Considering the crystal structure, the main magnetic interaction involves the gadolinium(III) ions and the imino-nitroxide radicals. Indeed the molecules are well isolated in the crystal and the intermolecular radical−radical interactions should be negligible. Furthermore both complexes show a slight inflection of the χT vs T curves about 10 K (ca. 6.3 emu K mol^{-1}), which is consistent with the expected value for a ground spin state $S = 3$ if the gadolinium and the radical are antiferromagnetically coupled (6 emu K mol^{-1}). At low temperature the decrease of χT may be assigned to weak intermolecular antiferromagnetic interactions.

As for complex **2a** the data were analyzed by a refinement program[43] diagonalizing the isotropic Hamiltonian ($H = -2\sum_{i<j} J_{ij}S_iS_j$) taking into account one Gd^{III}−radical (imino nitroxide) interaction (J_{Gd-rad}). The best fit of the experimental data gave $g = 2.02$ and $J_{Gd-rad} = -2.6$ cm^{-1} (**3a**), and $g = 2.02$ and $J_{Gd-rad} = -1.9$ cm^{-1} (**4a**) and $R = 5 \times 10^{-4}$. The antiferromagnetic Gd^{III}−radical coupling was confirmed by the magnetic field dependence of the magnetization, which reaches for both compounds (**3a** and **4a**) a saturation value close to 6 μ_B at 2 K (Figure 5), which is the value expected for a ground spin state $S = 3$.

Absorption and Luminescence Spectra. The series of complexes characterized as described in the previous sections provide an ideal situation for a detailed comparison of optical spectra. The effects of the different radical ligands, different lanthanide metal centers, and different ancillary ligands on absorption and luminescence spectra are described in the following.

Figure 6 shows the near-infrared luminescence spectrum of [$Gd^{III}(hfac)_3$NITBzImH] (**2a**) compared to the lowest energy absorption band. Even at 5 K, the luminescence spectrum is weak, but it shows well-resolved structure. Similar luminescence bands can be observed for many other complexes of trivalent lanthanides with radical ligands and also for the free radical ligands in the solid state. We choose

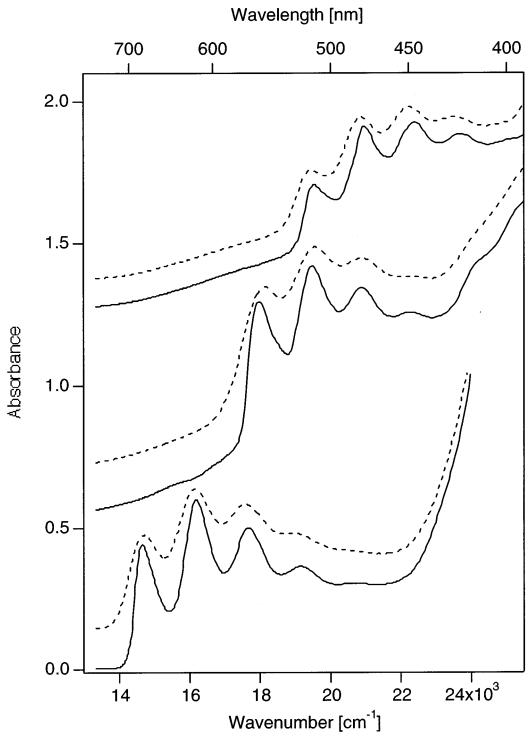

Figure 7. Absorption spectra of [$Gd^{III}(hfac)_3$(radical)] complexes (**2a**−**4a**). Solid lines denote spectra measured at 5 K; dotted lines, spectra measured at 290 K. Bottom spectra: **2a** (radical = NITBzImH). Middle spectra: **3a** (radical = IMBzImH). Top spectra: **4a** (radical = IMPy). Spectra are offset along the ordinate axis for clarity.

this example to identify systematically the relevant overall features found in all luminescence and absorption spectra of the title complexes. The luminescence spectrum in Figure 6 is, to the best of our knowledge, the first report of a full spectrum extending out into the near-infrared wavelength region. The highest energy peak for this and related compounds has been reported in a preliminary communication[38] and has also been observed for a chromium(III) complex with this ligand.[44] The full spectrum consists of a main progression with four members separated by an average interval of 1550 ± 15 cm^{-1}. Raman spectra and a vibrational analysis from the literature show that this interval is in good agreement with modes observed at approximately 1530 cm^{-1} [44] and is assigned as the stretching frequency of the ONC moiety of the radical ligand. At first glance, the absorption spectrum appears as a mirror image of the luminescence trace; it too consists of a progression with four members, although less resolved than the luminescence spectrum. The separations between absorption peaks are 1518, 1486, and 1452 cm^{-1}, starting from the lowest energy absorption maximum. This decrease is in marked contrast to the constant interval between peaks forming the luminescence spectrum.

Figure 7 shows that the energy of the first absorption band varies for Gd(III) complexes with different radical ligands, underlining again that the electronic transitions observed in the visible wavelength range are centered on the radical. The

(44) Tsukahara, Y.; Iino, A.; Yoshida, T.; Suzuki, T.; Kaizaki, S. *J. Chem. Soc., Dalton Trans.* **2002**, 181.

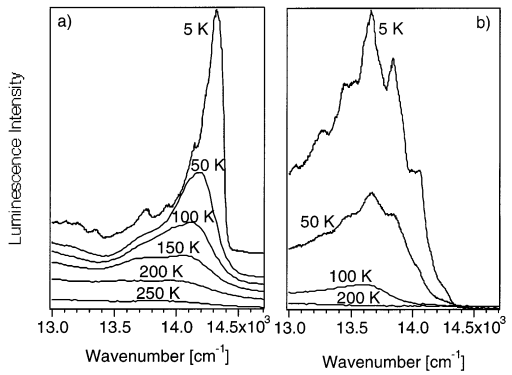

Figure 8. Temperature dependence of the highest energy luminescence band of $[Gd^{III}(hfac)_3NITBzImH]$ (**2a**). The full luminescence spectrum is shown in Figure 1. (b) Temperature dependence of the highest energy luminescence band of $[Gd^{III}(NITBzImH)_2(NO_3)_3]$ (**1a**). Spectra are offset along the ordinate axis for clarity.

lowest energy transition is observed for the complex (**2a**) of the blue nitronyl nitroxide radical NITBzImH (**5**), followed by those of the complexes (**3a** then **4a**) of the red imino nitroxide radicals IMBzImH (**6**) and IMPy (**7**), which show bands higher in energy than the NITBzImH ligand (**5**) by approximately 3000 and 5000 cm^{-1}, respectively. The spectra are less resolved at room temperature than at 5 K, but their overall band shape does not change dramatically, as illustrated by the comparisons in Figure 7. Molar absorptivities ϵ on the order of 500 M^{-1} cm^{-1} have been reported for some lanthanide complexes with IMPy ligands in solution at room temperature.[34]

It is surprising that the ligand-centered luminescence transitions show a distinct dependence on the number of radical ligands, the ancillary ligands, and the coordination number of the lanthanide ion. Figure 8 compares luminescence spectra for $[Gd(hfac)_3(NITBzImH)]$ (**2a**) and $[Gd(NITBzImH)_2(NO_3)_3]$ (**1a**). Only the highest energy band is shown. A clear-cut difference appears: the nitrato complex has a larger band, structured with a low-frequency progression with an average spacing of 190 ± 5 cm^{-1}, which is absent in the complex with hfac ligands. The hexafluoroacetylacetonato complex in Figure 8a shows a distinct red-shift of the band maximum with increasing temperature, whereas the nitrato complexes have a broader band at low temperature that does not change its shape, but becomes less resolved with increasing temperature. At temperatures above 100 K the spectra from both types of compounds become similar. No hot bands at energies higher than the onset of the luminescence spectrum at 5 K are observed at any temperature. The luminescence spectra of Eu(III) and Gd(III) complexes with the same ligand spheres are identical.

Figure 9 shows a comparison of luminescence spectra of a series of Eu(III) complexes. The Eu(III) ion shows a well-studied f−f luminescence corresponding to the $^5D_0 \rightarrow {}^7F_J$ electronic transition at energies between 16 000 and 16 500 cm^{-1}. Figure 9 illustrates that the luminescence behavior of the europium(III) compounds can be tuned through the choice of radical ligand. Compounds **1b** and **2b** with NITBzImH radical ligands absorbing at low energies show the broad luminescence given as top traces in Figure 9. For compounds

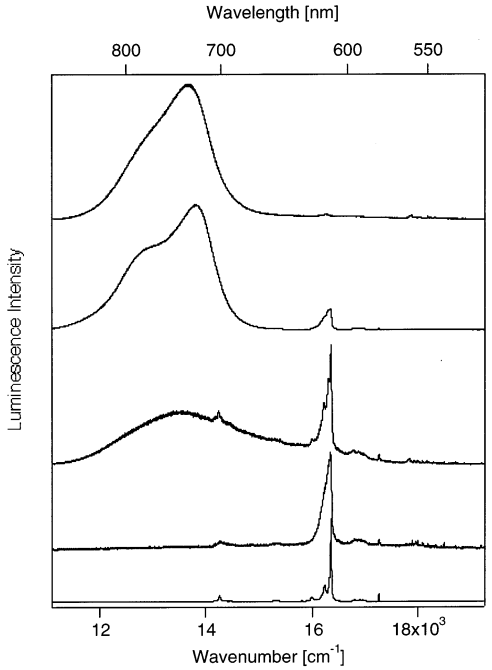

Figure 9. Comparison of luminescence spectra of Eu(III) complexes with radical ligands. Top to bottom: $[Eu^{III}(NITBzImH)_2(NO_3)_3]$ (**1b**) (290 K), $[Eu^{III}(hfac)_3NITBzImH]$ (**2b**) (290 K), $[Eu^{III}(hfac)_3IMBzImH]$ (**3b**) (5 K), and $[Eu^{III}(hfac)_3IMPy]$ (**4b**) (5 K). The lowest trace is $Eu(hfac)_3 \cdot 2H_2O$ (5 K) and gives the spectrum of the metal-centered transition for a complex without radical ligands.

3b and **4b**, whose radical ligands have excited states at higher energy, the luminescence from the Eu(III)-centered transition dominates, as shown in the bottom half of Figure 9. Luminescence centered on the europium(III) ion with an IMPy ligand confirming our results was recently reported.[34] These spectroscopic results illustrate the wide range of luminescence properties displayed by the title compounds.

Discussion

Synthesis, Structural Aspects, and Magnetic Properties. Complexes **1a**−**4a** and **1b**−**4b** were all recovered as single crystals with yields superior to 65%, from the mixture of the radical with $[Ln(NO_3)_3 \cdot 6H_2O]$ in ethanol (**1a** and **1b**) or with $[Ln(hfac)_3 \cdot 2H_2O]$ in heptane−chloroform solutions (**2a**−**4a** and **2b**−**4b**). The compounds were found stable for long periods of time.

Along the series, each gadolinium(III) complex (**1a**−**4a**) is isostructural with the europium(III) analogue complex (**1b**−**4b**).

A remarkable characteristic of the imino nitroxide complexes is that, similar to d-block transition metal ions,[45−47] the rare earth ions are bound to the imino nitrogen (N1) atom, instead of the NO oxygen atom (O1), as could be anticipated from their well-known oxophilicity. This could be due to the weak Lewis basicity of the NO oxygen atoms and that coordination to the imino nitrogen atom allows a better

(45) Luneau, D.; Rey, P.; Laugier, J.; Belorizky, E.; Cogne, A. *Inorg. Chem.* **1992**, *31*, 3578.
(46) Luneau, D.; Rey, P.; Laugier, J.; Fries, P.; Caneschi, A.; Gatteschi, D.; Sessoli, R. *J. Am. Chem. Soc.* **1991**, *113*, 1245.
(47) Rey, P.; Luneau, D.; Cogne, A. *NATO ASI Ser., Ser. E* **1991**, *198*, 203.

minimization of the steric constraints [Gd−N1 2.599(5) Å (**3a**), Gd−N1 2.555(2) Å (**4a**), Eu−N1 2.621(2) Å (**3b**), Eu−N1 2.557(2) Å (**4b**)] in comparison with coordination through the NO oxygen atom [Gd−O1 2.342(3) Å (**2a**) and Gd−O1 2.322(7) Å[19]].

Among the gadolinium(III) complexes of the series **1a**−**4a** only [Gd(hfac)$_3$NITBzImH] (**2a**) exhibits a ferromagnetic Gd^{III}−radical interaction, while the imino nitroxide complexes [Gd(hfac)$_3$(radical)] [(radical = IMBzImH (**3a)** and IMPy (**4a**)] are two novel examples of antiferromagnetic Gd^{III}−radical interactions.

Looking at the structural features, no clear trend is observed. When comparing the [Gd(hfac)$_3$radical] series (**2a**−**4a**), the apparent trend is that the Gd^{III}−radical coupling becomes more antiferromagnetic as the Gd^{III}−radical distance increases [**2a**: $J_{Gd-rad} = +1.7$ cm^{-1}, Gd−O1(NO) = 2.342(3) Å; **3a**: $J_{Gd-rad} = -2.6$ cm^{-1}, Gd−N1(imino) = 2.599 Å; **4a**: $J_{Gd-rad} = -1.9$ cm^{-1}, Gd−N1(imino) = 2.555(4) Å]. This is no more strictly the case when comparing them to the nitrato complex [Gd^{III}(NITBzImH)$_2$(NO$_3$)$_3$] (**1a**: $J_{Gd-rad1} = -4.05$ cm^{-1} and $J_{Gd-rad2} = -0.80$ cm^{-1}, Gd−O1A(NO) = 2.405 cm^{-1} and Gd−O1B(NO) = 2.365(3) Å). It does not work at all when comparing the nitrato complex **1a** to structurally similar compounds reported by Sutter et al., but with different radicals and a ferromagnetic Gd^{III}−radical coupling.[20,48] Here the trend is that the Gd^{III}−radical coupling becomes ferromagnetic when the Gd^{III}−radical bond length increases [Gd−O1 2.460(15) Å and Gd−O4 2.430(15) Å, $J_{Gd-rad} = +6.1$ cm^{-1}].[20] These observations indicate that the sign and magnitude of the Gd^{III}−radical interactions depend on the detailed electronic structure and on bonding characteristics involving the lanthanide ions, the radical ligands, and the ancillary ligands.

Assignment of the Emitting State and the Lowest Energy Absorption Band. The full luminescence spectrum in Figure 6 indicates directly that the ground and emitting states have different structures in the regions of high unpaired electron density of the radical ligands, because a vibronic progression involving the NCO mode is observed. This observation is in qualitative agreement with the n → π^* assignment typically given for the corresponding absorption band in the literature.[35] There appear to be shoulders on the peaks forming this progression, but the signal-to-noise ratio does not allow a detailed analysis. The comparison of spectra from a variety of lanthanide complexes, given in Figures 6, 8, and 9, clearly shows that the transition is ligand centered, even though this was doubted in a recent study.[44] The overlap in the area of the electronic origin in Figure 6 is evidence that the observed luminescence does not arise from traps. The partial spectra presented in detail in Figure 8 show that the nature of the complex has a definite influence on the emitting state. The sequence of bands observed for the nitrato complexes is absent in the spectra of the free ligand[38,49] and is caused most likely by a vibronic effect. We exclude a magnetic phenomenon because a very similar effect has been observed for the La(III) nitrato analogue, where no metal−radical magnetic coupling can occur.[38,49] The comparison of luminescence spectra for Eu(III) complexes in Figure 9 shows very clearly that the title compounds always emit from the lowest energy excited state. The change from radical-centered to metal-centered luminescence further corroborates the character of the broad luminescence as arising from a transition centered on the radical.

The spacing between peaks in the lowest energy absorption band system is irregular, as shown in Figure 6. The intensity distribution does not correspond to a mirror image of the luminescence band, where the first member of the progression is most intense. It is therefore very unlikely that the absorption band system corresponds to a single excited state. Detailed MO calculations on the ligands have shown that the energy differences between SOMO-1, SOMO, and SOMO+1 are of similar magnitude, leading therefore to one-electron excitations that are close in energy.[49] We therefore conclude that the absorption band systems in Figures 6 and 7 correspond to at least two overlapping transitions, confirmed experimentally by the highly resolved spectra of the crystalline cyano nitronyl-nitroxide (NITCN).[50] The variation of the absorption band centered on the radical for the three Gd(hfac)$_3$(radical) complexes (**2a**, **3a**, and **4a**) shown in Figure 7 illustrates that all overlapping bands shift in energy for a different radical.

Qualitative Correlations between Optical Spectra and Magnetic Properties. In contrast to a large number of d-block complexes with exchange coupling between paramagnetic metal centers, where ground state exchange splittings can be directly determined from luminescence spectra,[51] no such energy differences appear directly in our spectra. This is not unexpected for lanthanide ions, as the exchange effects are much weaker than those of the d-block elements, illustrated by the magnetic measurements presented for selected compounds in Figures 6 and 7. It is nevertheless interesting to examine if spectroscopic trends such as energy differences can be at least qualitatively correlated to the sign of the metal−radical exchange interaction.

Two qualitative correlations are striking:

First, the luminescence spectra in Figures 8 show distinct differences between complexes with two (**1a** and **1b**) or only one radical ligand (**2a** and **2b**). The spectra of the nitrato complexes (**1a** and **2b**) with two radical ligands and a clearly visible progression illustrated in Figure 8b show an antiferromagnetic gadolinium−radical coupling. This progression indicates a significant distortion along a low-frequency normal coordinate at all temperatures, likely involving radical−lanthanide−radical modes, as it is not observed for complexes with only one radical ligand or for uncoordinated radicals.[38] On the other hand, the narrow low-temperature spectra in complexes **2a** and **2b** with only one radical ligand are linked to ferromagnetic interactions. At higher temper-

(48) Kahn, M. L.; Sutter, J.-P.; Golhen, S.; Guionneau, P.; Ouahab, L.; Kahn, O.; Chasseau, D. *J. Am. Chem. Soc.* **2000**, *122*, 3413.
(49) Beaulac, R.; Bussière, G.; Reber, C.; Lescop, C.; Luneau, D. (submitted) **2002**.
(50) Hirel, C.; Luneau, D.; Pécaut, J.; Öhrström, L.; Bussière, G.; Reber, C. *Chem. Eur. J.* **2002**, *8*, 3157.
(51) McCarthy, P. J.; Güdel, H. U. *Coord. Chem. Rev.* **1988**, *88*, 69.

atures, the luminescence spectra of these compounds become broader, indicating that a vibronic effect involving a low-frequency lanthanide−radical coordinate similar to complexes **1a** and **2a** could determine the band shape. Such an effect would lead to a red-shift of the band maximum, as observed in Figure 8a, and is a first observation showing that bonding properties in these compounds are temperature dependent. In view of the weak exchange interactions, the magnetic order is lost at higher temperatures, as illustrated in Figures 4 and 5, and the similarities of the spectra in Figure 8 at temperatures above 50 K are not likely to influence the magnetic properties at very low temperatures. The different low-temperature band shapes in Figure 8 indicate that antiferromagnetic coupling dominates in complexes where a low-frequency progression is observed and is possibly promoted by this vibronic effect. A narrow band without this progression appears to be observed for ferromagnetic lanthanide−radical coupling.

Second, within the [$Gd^{III}(hfac)_3$radical] series (**2a**−**4a**), where only the radical changes, the lanthanide−radical coupling becomes antiferromagnetic as the lowest energy absorption bands shift to higher energy, illustrated in Figure 7. It is not straightforward to quantitatively rationalize this trend, but it underlines the importance of interactions or mixing of excited states into the ground state,[26] an effect that becomes weaker as the energy separation between the ground and the excited states of the radical increases. The relatively small change of the absorption energy in Figure 7 by 3000−5000 cm^{-1} is sufficient to go from ferromagnetic to antiferromagnetic coupling for the three related complexes in Figure 7. Thus the Gd^{III}−radical coupling changes from ferromagnetic to antiferromagnetic when the blue nitronyl nitroxide radical NITBzImH (**5**) is replaced by the red imino nitroxide radical IMBzImH (**6**). The results presented here allow us to conclude that both the energy difference between ground and emitting states and the detailed band shape of the luminescence spectra can be qualitatively correlated with the sign of the lanthanide−radical exchange interaction.

An appealing suggestion is that in some cases the energy difference between the singly occupied orbital of the radical (SOMO) and the empty 5d orbital on the gadolinium(III) center leads to an increase of the SOMO to 5d electron transfer energy, which was previously postulated to be a determining factor for the ferromagnetic Gd^{III}−radical [or Cu^{II}−Gd^{III}] interaction.[26] If this energy increases sufficiently, the magnetic interaction becomes antiferromagnetic.

More extended optical spectroscopic measurements, including absorption spectra of charge transfer bands in the ultraviolet region, are necessary to reliably establish magnetic properties from spectra, but the qualitative trends obtained from our results allow at least an approximate prediction for new compounds. The spectroscopic information provides insight on electronic structure and magnetic properties even in the absence of resolved bands corresponding to exchange splitting patterns.

Acknowledgment. This work was supported in France by the Centre National de la Recherche Scientifique (CNRS), the Commissariat à l'Energie Atomique (CEA), the Grenoble University (UJF), and in Canada by the Natural Sciences and Engineering Research Council. We thank the Centre Jacques Cartier and the Commission Permanente de Coopération Franco-Québécoise for support through travel grants.

Supporting Information Available: Crystallographic data for compounds **1a**−**4a** and **2b**−**4b** in CIF format. View of the molecular structure of **3a** and **4b**. Selected bond lengths and angles for compounds **1a** and **1b**. Temperature dependence of χT for compounds **1a** and **4a**. This material is available free of charge via the Internet at http://pubs.acs.org.

IC0257928